Soft Science

Review Article

Soft wearable electronics for evaluation of biological tissue mechanics

Yifei Lu[1,#], Lichao Ma[1,#], Hehua Zhang[2,#], Yongfeng Mei[1,3,4], Ze Xiong[5,6,7], Enming Song[1,3,4,*]

[1]Institute of Optoelectronics, Shanghai Frontiers Science Research Base of Intelligent Optoelectronics and Perception, State Key Laboratory of Integrated Chips and Systems (SKLICS), Fudan University, Shanghai 200438, China.
[2]Department of Biomedical Engineering, City University of Hong Kong, Hong Kong 999077, China.
[3]International Institute for Intelligent Nanorobots and Nanosystems, Fudan University, Shanghai 200438, China.
[4]Yiwu Research Institute of Fudan University, Yiwu 322000, Zhejiang, China.
[5]Wireless and Smart Bioelectronics Lab, School of Biomedical Engineering, ShanghaiTech University, Shanghai 201210, China.
[6]State Key Laboratory of Advanced Medical Materials and Devices, ShanghaiTech University, Shanghai 201210, China.
[7]Shanghai Clinical Research and Trial Center, Shanghai 201210, China.
[#]Authors contributed equally.

[*]**Correspondence to:** Prof. Enming Song, Institute of Optoelectronics, Shanghai Frontiers Science Research Base of Intelligent Optoelectronics and Perception, State Key Laboratory of Integrated Chips and Systems (SKLICS), Fudan University, Jiangwan Campus, 2005 Songhu Rd., Shanghai 200433, China. E-mail: sem@fudan.edu.cn

Abstract

Flexible wearable devices designed to evaluate the biomechanical properties of deep tissues not only facilitate continuous and effective monitoring in basic performance but also exhibit significant potential in broader disease assessments. Recent advancements are highlighted in the structural and principled design of platforms capable of capturing various biomechanical signals. These advancements have led to enhanced testing capabilities concerning spatial scales and resolution modes at different depths. This review discusses the engineering of soft wearable devices for the biomechanical evaluation of deep tissue signals. It encompasses different measurement modes, device design and fabrication methods, integrated circuit (IC) integration schemes, and the characteristics of measurement depth and accuracy. The core discussion focuses on platform development, targeting different monitoring sites and platform structure design, ranging from linear strain gauges and conformal stretchable sensors to complex three-dimensional (3D) circuit-integrated stretchable arrays. We further explore various technologies associated with different measurement mechanisms and engineering designs, as well as the penetration depth and spatial resolution of these wearable sensors. The practical applications of these technologies

are evident in the monitoring of deep tissue signals and changes in tissue characteristics. The results suggest that wearable biomechanical sensing systems hold substantial promise for applications in healthcare and research.

Keywords: Wearable devices, passive electrodes, active recording, deep-tissue sensing

INTRODUCTION

Employment of digital health and wearable technologies potentially revolutionizes diagnostic and therapeutic approaches, offering robust support to the healthcare ecosystem[1-4]. Of particular interest with epidermal electronics are their mechanical properties (geometries, flexibility/stretchability and unique form factors), allowing conformal contact with skin and living tissues, thereby quantifying the biological tissue mechanics in a higher signal-to-noise ratio[5-9]. Unique emphasis on the measurement of elastic moduli forms the foundation for healthcare appraisals to assess physiological health status regarding intraocular pressure[10,11], dermatological pathologies[12], and cardiovascular status[13]. Furthermore, wearable devices designed for monitoring physiological health continuously demonstrate accuracy and reliability equivalent to high-end wired systems utilized in intensive care units, while maintaining cost-effectiveness, adaptability and portability across various environments, including hospitals, work environments, and home environments.

Conventional methods to determine tissue moduli consider the non-linear stress-strain relationship based on the applied force (such as torsion, compression, suction, and indentation) and the dynamic nature of the tissue[4,14-16]. Normal tissues have varying hardness when assessed on the same strain and temporal scales. The brain is incredibly soft, having an elastic modulus of around 100 Pa; the liver, while also very soft, is slightly harder at 400-600 Pa. Medical practice dictates that tissue hardness changes in response to illness. Several investigations show that fibrotic lungs harden during fibrosis, with elastic modulus values ranging from around 2 kPa in normal tissue to about 17 kPa in fibrotic tissue[17]. We discovered that the shear modulus of normal liver *in vitro* is less than 1 kPa, whereas the shear modulus of fibrotic liver ranges from 3 to 22 kPa[2,17]. The emphasis on measuring the elastic modulus of tissues aids in the evaluation of various pathological and physiological conditions[2,17]. Typically, these methods involve the utilization of external equipment in an invasive manner; however, when applied *in vivo*, substantial variations play a crucial role in influencing the outcomes under different experimental conditions[18]. Simultaneously, the emergence of novel testing methods, such as magnetic resonance elastography (MRE)[19] and ultrasound elastography[18], has come to fruition. Ultrasound elastography, which combines both backscattered and through-transmission data, shows a comprehensive method to estimate soft tissue elasticity associated with the bulk modulus as well as shear and Young's moduli to reach deeper tissues (approximately 10 cm depth)[18,20]. The most recently used dynamic elasticity imaging techniques exploit MRE[21] for non-invasively mapping the viscoelastic properties of soft biological tissues in the extensive diagnostic applications of magnetic resonance imaging (MRI). MRE offers parameter distributions with high spatial resolution ranging from millimeters to sub-millimeters[21] to picture various mechanical functions and structural characteristics of pathological changes in tissues[19]. However, these high-priced instruments demand careful configuration and specialized hospital/lab professionals, thus impeding their swift, direct application for household diagnostic monitoring or continuous tracking.

Recently developed wearable system categories include ultra-thin, flexible actuator/sensor arrays, which are becoming increasingly interesting as conceptually different types of methods for measuring soft tissue biomechanical signals with unique form factors[22-26]. Key points primarily involve precise measurements at the microscale and in wearable formats, including dimensions of micro-devices, mechanical formats, and adhesion strength to biological surfaces[27]. It explores possibilities to enhance spatial and temporal

resolution in near-surface depth measurement and minute deformation measurement of soft tissues through methods such as piezoelectric actuation[28,29], ultrasound arrays[18,20], and optical coherence elastography (OCE)[30,31].

Understanding the generation and feedback of signals in superficial tissues can aid in evaluating the health status of deeper tissue organs. Firstly, it offers a better understanding of the biomechanical responses of tissues under conditions of both health and degradation, contributing to the explanation of tissue behavior[2,32]. For example, changes in skin mechanical signals can be used to monitor skin diseases such as scleroderma and psoriasis. Secondly, it helps characterize the mechanical properties of soft tissues, which play a crucial role in physiology and disease[33]. Lastly, it enables the evaluation of tissue characteristics at different scales[34], such as detecting changes in intraocular pressure through eye monitoring signals and reflecting cardiovascular status by seizing blood pressure (BP) waveforms from deep-seated vessels[35-40]. Overall, mechanical measurement of biological tissues is crucial for advancing the understanding of tissue mechanics, disease processes, and treatment strategies.

In this review, we discuss essential strategies for soft wearable devices for the evaluation of biological tissue mechanics, which are focused on characterizing the mechanical properties of soft biological tissues in various locations [Figure 1]. The emphasis is on the systematic properties of engineering designs and methodologies, which possess diagnostic utility across varying measurement depths. This article commences with an outline of multiple categories of wearable devices, ranging from flexible threads to stretchable devices and three-dimensional (3D) circuit integrators. Secondly, microelectromechanical devices are utilized for profound analysis of soft tissue biomechanics at adjustable characteristic depths, ranging from shallow skin to mid to deep organ signal acquisition. Finally, examples will be given to explain its applications, such as monitoring alterations in tissue mechanical properties and targeting anomalous areas related to various diseases. These applications include voice code recognition[41], dermatologic malignancy evaluation[29], arterial stiffness measurement[20], neonatal physiological monitoring[20], and more. Recent advancements in these areas have the potential to transform tissue mechanics monitoring into a significant aspect of healthcare and biomedical research, which are crucial for early diagnosis, monitoring disease progression, and guiding treatment strategies in various medical fields.

EMERGING CLASSES OF SOFT WEARABLE DEVICES TO CAPTURE HUMAN BODY MECHANICS

Overview of different sensing platforms for biological tissue mechanics with unique form factors

This section focuses on the biomechanics-sensing strategies of wearable microsystem technology for mechanical measurement in biological tissues, which rely on small deformations of tissues, such as intraocular pressure[10,11], vocal cord vibration[42], heartbeat[43], muscle movement[44], changes in biological tissue mechanical properties[28,29], and pulse pulsation[20] [Figure 1A]. When designing for clinical or home use, reliability and high measurement accuracy are essential considerations. The goal of wearable engineering is often to miniaturize size, conform to design and tissue mechanics, and match or continuously connect with biological targets within short time intervals. The focus here is on providing a measurement platform for mechanical compliance for the target organization.

Recent examples include strain gauges with filaments [Figure 1B][10], stretchable electronic platforms with biological compliance [Figure 1C][45], and 3D circuit integrations for deep tissue characterization [Figure 1D][46]. Conventional rigid devices rely on numerous displacement measurements in response to large applied loads, leading to uncertainties during measurement and challenges when applied to bending tissue surfaces that change over time. These microsystems, characterized by tissue-like mechanics, possess a
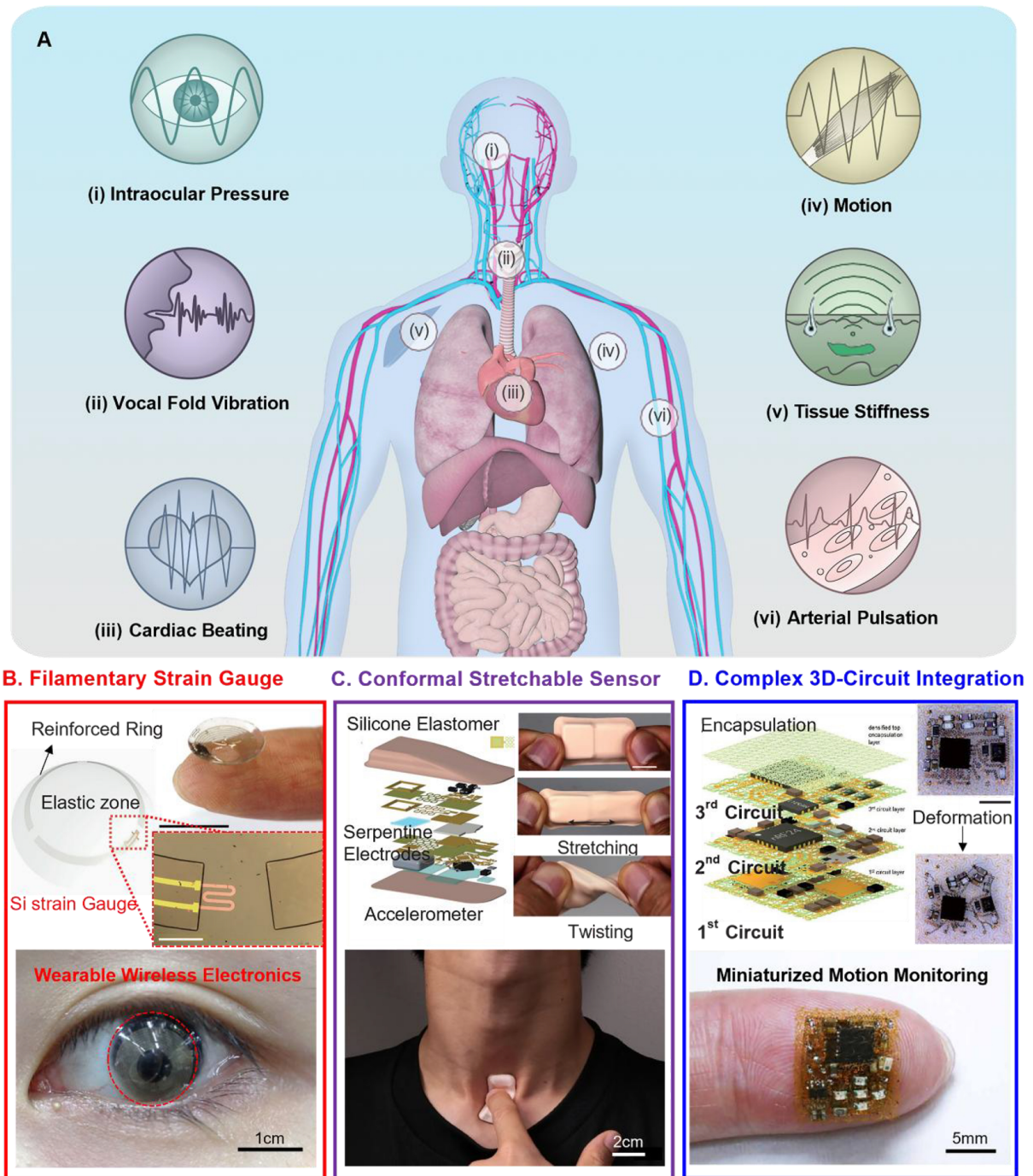
Figure 1. Overview of different sensing platforms with unique form factors. (A) Six major categories of soft tissue biomechanical signals that can be detected by wearable sensing platforms; (B) Filamentary strain gauge resting on the contact lens for quantitative monitoring of IOP placed on the human eye. Reproduced with permission[10]. Copyright 2022, Springer Nature; (C) Photograph of conformal stretchable sensing interfaced to the suprasternal notch for mechano-acoustic signatures of body processes. Reproduced with permission[45]. Copyright 2019, Springer Nature; (D) Optical image of SMNM-based electronic system consisting of stretchable 3D-stacked ICs and serpentine interconnects mounted on the index finger. Reproduced with permission[46]. Copyright 2022, Springer Nature. IOP: Intraocular pressure; SMNM: stacked multilayer network materials; 3D: three-dimensional; ICs: integrated circuits.

unique flexible and stretchable form, enabling stable measurements through a minimally invasive interface with biological surfaces.

The manufacturing technologies used in the integrated circuit (IC) industry can serve as the basis for the manufacture of devices in part or in full. Figure 1B illustrates the use of filamentary tissue microsystems for intraocular pressure measurement[10]. The contact lens features a strain sensor (p-type Si, 300 nm thick), a strain-concentrating layer, a AgNF wireless antenna with an average diameter of 432 ± 35 nm, capacitors, resistors, and an IC chip designed with stretchable electrical interconnects made from 3D metal structures (EGaIn ink, comprising 75.5% gallium and 24.5% indium alloy by weight). Stretchable interconnect circuits are printed on EGaIn ink in the x-y plane at a speed of 0.2 mm·s⁻¹ and 30 p.s.i., and in the z-direction, printing is accomplished by moving 0.001-0.01 mm·s⁻¹ with an ink volume of 3 p.s.i. When the intraocular pressure changes, the adjacent contact tissue experiences small-scale mechanical deformation, which is reflected by the change in the tensile strain of the silicon[47].

Multilayered structural design can achieve highly effective shape retention against bodily changes and can cover large flexible surfaces in a non-penetrative manner for wearable systems[48]. A representative example is shown in Figure 1C. Here, advanced microsystems based on accelerometers and electronic stethoscopes used for mechanical vibration sensing also have the ability to generate information about the biomechanical characteristics of biomolecular targets[45]. The inertia of the mass block in an accelerometer induces deformation of the piezoelectric material, generating a voltage that is proportionate to the inertial force, thereby turning acceleration into an electrical output. Accelerometers can detect a wide range of signals and simultaneously capture multiple vibrations, from low-frequency body direction (0.1 Hz) to high-frequency vocal cord vibration (> 100 Hz); however, they are limited in their ability to distinguish between vibrations in overlapping frequencies. The flexible printed circuit board (fPCB) of this device is supported by a 25 μm thick polyimide (PI) layer, with 12 μm thick annealed copper (Cu) traces on the top and bottom surfaces, all encapsulated with a PI insulation layer (25 μm, FR 1510, DuPont). The electronic subsystems in the circuit include a three-axis digital accelerometer (BMI160, Bosch), a microcontroller (nRF 52832, Nordic Semiconductor), and a wireless induction charging circuit. Further advanced signal processing techniques should be applied on the precise measurement of tissue mechanics.

Key indicators of stretchable inorganic electronic devices are elastic stretchability and functional density[49]. As shown in Figure 1D, stacked multilayer network materials as a universal platform allow for the interconnection of individual components and stretchability without being constrained by deformation[46]. The system consists of a periodic triangular lattice of a horseshoe-shaped microstructure composed of stretchable interconnects and soft network materials (PI; 50 μm thick), and the serpentine interconnects are realized by three hollow pads (3.3 μm PI / 0.8 μm Cu / 3.3 μm PI). Multifunctional flexible electronics were developed, featuring approximately 20% elastic stretchability and around 110% IC coverage. This system achieves high-precision sensing of temperature, humidity, and degree of freedom of movement, as well as wireless radio frequency (RF) transmission. The demonstration of synchronously capturing physiological signals highlights its wide range of potential applications. Additionally, the high IC coverage facilitates the integration of wireless data transmission capabilities and supports a battery-free design, making it suitable as a skin-mounted platform for wearable diagnostics.

As mentioned above, for the monitoring of deep physiological signals, microsystem technology is of particular interest due to its flexible/stretchable mechanics and miniaturized size, with consequences including the realization of corresponding sensing depths and spatial and temporal resolutions in the case of precise measurements and continuous monitoring. These features suggest potential uses in deep tissue signal monitoring that can be achieved with microsystems[50].

Measurement mechanisms and engineered designs

Active vibration sensor

Passive or active mechanical sensing can effectively capture deep tissue movements. The principle of active mechanical sensing involves applying external loads to study their mechanical responses[51]. The modulus of adjacent contacting tissues can be determined by analyzing data obtained after applying voltage to the mechanical actuator and measuring the induced voltage at the sensor [Figure 2A]. In the example of Figure 2B, microelements (dimensions 200 μm × 140 μm, spaced 1 mm apart) composed of piezoelectric material lead zirconate titanate (PZT) provide both mechanical actuation (far from the tip) and sensing (near the tip)[28]. Active elements consist of patterned multilayer stacks of PZT (500 nm) between bottom (Ti/Pt, 5/200 nm) and top (Cr/Au, 10/200 nm) electrodes. Piezoelectric microsystems provide a foundational design tool for rapid modulus-based characterization of tissues[29,42]. The dependence of the sensor voltage on tissue modulus is non-monotonic. In the low modulus state, the free deformation of the actuator and substrate makes their response highly localized, which results in a small strain generated in the sensor and a correspondingly small voltage output. In the high modulus state, the mechanical load limits the deformation of the actuator and substrate, which also leads to a smaller sensor voltage. A standard law (1) is used to correlate the tissue modulus E_{tissue} with the sensor voltage V_{sensor}:

$$\frac{V_{sensor}}{V_{actuator}} = \frac{e_{31}^2 A_{PZT} h_{PZT}}{k_{33} E_{PI} h_{PI} d^2} G\left(\frac{E_{tissue} d^3}{E_{PI} h_{PI}^3}\right) \tag{1}$$

where $V_{actuator}$ is the actuator voltage, e_{31} is the piezoelectric coefficient, k_{33} is the dielectric coefficient, and E_{PI} is the modulus of a needle-like substrate made of PI; other geometric parameters include thickness h_{PZT}, area A_{PZT}, thickness h_{PI} and spacing d between the actuator and sensor. Based on the principles of elastic imaging, the potential of biopsy-guided miniaturized modulus sensing devices is demonstrated in this work, proving the feasibility of detecting hepatocellular carcinoma (HCC) in liver tissue.

Ultrasonography

Ultrasound is a special form of active vibration sensing with frequencies ranging from 20 kHz to 200 MHz[51]. Ultrasound waves can propagate in tissues with almost no damping, and when sound waves encounter tissues with different acoustic impedances, they rebound and carry anatomical patterns and mechanical information of deep tissues. In an ultrasound system [Figure 2C], transducers generate and receive ultrasound waves. As shown in Figure 2D, the array includes 12 × 12 ultrasound transducers (unit area of 550 × 550 μm², thickness of 600 μm, and pitch of 770 μm), where the transducers are composed of 1-3 piezoelectric composite elements formed by cutting and filling technology[52]. Each transducer is electromechanically coupled to the skin in a way that electrical power is effectively converted into vibration power through phased array control technology, which can achieve signal monitoring in deep tissue areas (about 14 cm below the skin) with negligible degradation in signal quality (signal-to-noise ratio > 18 dB). The stretchable phased array is placed on the neck of the human body and the ultrasound beam is focused and steered to measure blood flow in the carotid artery (CA) and adjacent jugular vein. Phased-array transmit and receive beamforming maximizes the ultrasonic energy scattered by these red blood cells, allowing for more accurate and reliable computation of blood flow signals. By extracting Doppler frequency shift and blood vessel direction, the blood flow velocity is calculated by[53]

$$V = \frac{c f_d}{2 f_0 \cos\theta} \tag{2}$$
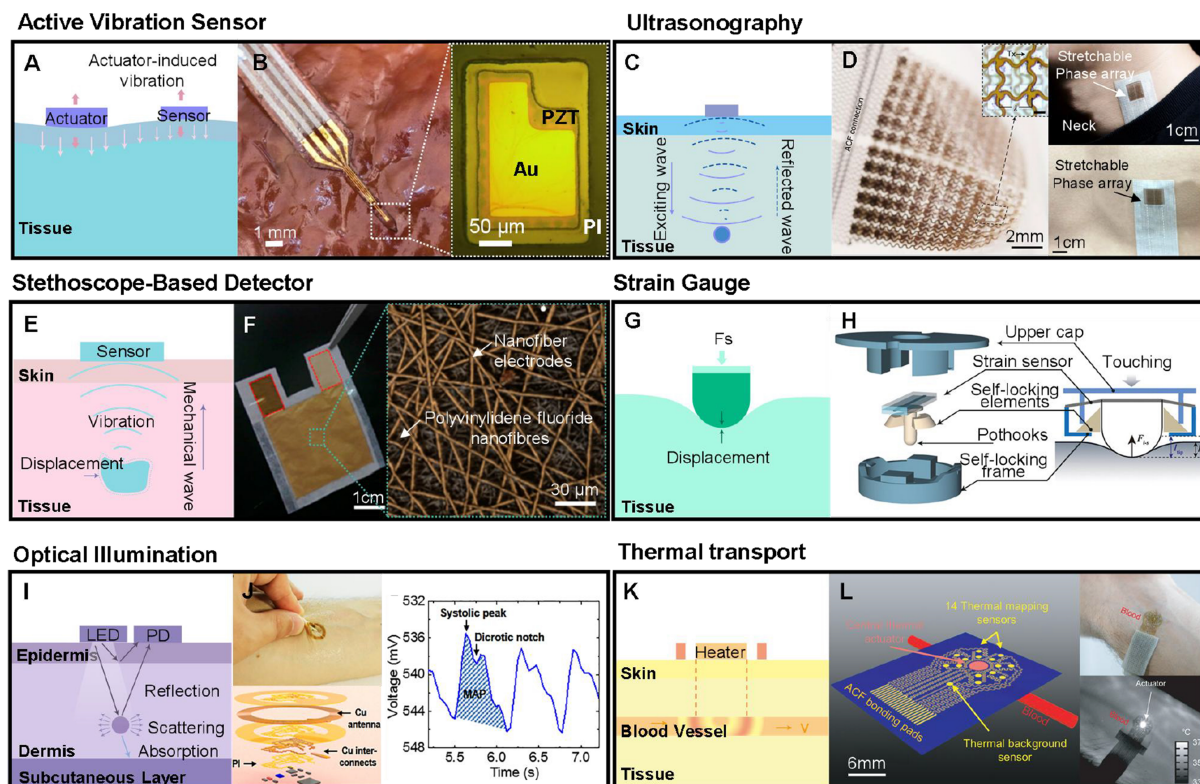
Figure 2. Various measurement mechanisms and engineered designs. (A) Active vibration sensors for tissue stiffness evaluation. Vibration generated by the actuator propagates along the tissue to the sensor; (B) Example of an ultrathin microsystem with active elements consisting of PZT, bottom and top electrodes, and PI for distinguishment of abnormal tissue. Reproduced with permission[28]. Copyright 2018, Springer Nature; (C) Working principle of ultrasonography for the detection of tissue signals; (D) Optical image of a 12 × 12 stretchable ultrasonic phased array mounted on the human neck and chest. Inset: enlarged image of four transducer (Tx) elements with a pitch (λ) of 0.8 mm. Reproduced with permission[52].Copyright 2021, Springer Nature; (E) Stethoscope-based mechanism for monitoring signals from tissue displacement; (F) Optical photograph (left) and microscopic image (right) of an ultrasensitive all-nanofiber mechanoacoustic sensor based on nanofibre electrodes and polyvinylidene fluoride nanofibres. Reproduced with permission[54].Copyright 2020, American Chemical Society; (G) Schematic showing the architecture of a strain sensor to measure haptically Young's modulus; (H) Illustration of a FMS with a self-locking effect composed of an upper cap, a strain sensor, a pair of self-locking elements, and a self-locking frame. Reproduced with permission[55].Copyright 2021, John Wiley and Sons; (I) Schematic illustration of light absorption detected through a LED and a PD for photonic diagnostics; (J) Image and exploded-view illustration of thin and stretchable optoelectronic systems including IR LED, a photodetector, and an inductive coil configured to measure cardiac beating signals with clear revelation of the systolic peak and the dicrotic notch. Reproduced with permission[31].Copyright 2016, American Association for the Advancement of Science; (K) Techniques based on thermal transport for continuous and precious measurements of blood flow; (L) The geometry of an electronic device combined with thermal analysis techniques consisting of a central thermal actuator (3 mm diameter) with power (typically 25 or 3.5 mW·mm^{-2}) directionally downstream to vessels and 14 surrounding thermal sensors for measurement of thermal distribution. Reproduced with permission[63].Copyright 2015, American Association for the Advancement of Science. PZT: Piezoelectric material lead zirconate titanate; PI: polyimide; FMS: fingertip modulus sensor; PD: photodetector; IR LED: infrared light-emitting diode.

where V is the blood flow velocity, c is the ultrasonic wave velocity in human tissue (~1,540 m·s^{-1}), f_d is the Doppler shift, f_0 is the center frequency of the transducer, and θ is the Doppler angle between the beam and the blood vessel. Moreover, this approach could enhance perfusion monitoring and allow continuous surveillance of at-risk organs in various patients.

Stethoscope-based detector

A stethoscope is a passive vibration sensor [Figure 2E]. Deep tissue vibrations that reach the skin surface can be captured by an electronic stethoscope, where the diaphragm vibrates and converts these movements

into electrical signals using piezoelectric or triboelectric materials. Wearable stethoscopes can incorporate nanostructured materials, such as a nanofiber electronic stethoscope [Figure 2F][54]. This sensor features a layer of polyvinylidene fluoride nanofibers situated between two nanofiber electrodes, with a gap (thickness of 5-15 μm) between the bipolar electrodes. The multilayered nanofiber sensor structure generates large vibration under the action of sound waves, making an acoustic sensitivity of up to 1 as high as 10,050.6 mV·Pa^{-1} in the frequency range of 10 to 500 Hz, which allows for continuous measurement of mechanoacoustic cardiac signals for longer periods of time (> 10 h) with an ultra-high signal-to-noise ratio of 40.9 dB.

Strain gauge
The self-locking stretchable strain sensor provides a fingertip measurement platform for the rapid detection of Young's modulus of soft materials (kPa-MPa) [Figure 2G]. The platform introduces the self-locking effect in the Hertz model to design a single stretchable strain sensor to achieve fingertip touch, avoiding the bulky displacement feedback systems typically required in conventional methods [Figure 2H][55]. The platform can measure the sample with just a simple contact, without considering the measurement process, which means that the fingertip modulus sensor (FMS) can quickly measure Young's modulus anytime and anywhere. The Young's modulus of the sample E_s can be defined as:

$$E_s = \frac{3}{4}\,(1 - v_s^2)F_{i-s}r_i^{-\frac{1}{2}}h_s^{-\frac{3}{2}} \tag{3}$$

where v_s is the Poisson's ratio of the sample and is a constant (≈ 0.5 for nearly incompressible materials), F_{i-s} is the contact force between the tip and the sample, r_i is the tip radius, and h_s is the sample deformation. To measure the contact force F_{i-s}, resistive stretchable strain sensors are set on the tip and the self-locking frame; F_{i-s} at any moment can be measured from the strain (ε) of the strain sensor. For the same material, the same resistance is generated regardless of the touch, while for different materials, distinct resistances are obtained. Portable Young's modulus measurements have a wide range of applications, such as evaluating the effects of drugs on swelling or cancer progression, and miniaturized sensing can be integrated on a large scale for the mechanical characterization of tissues[56,57].

Optical illumination
The optical system in the active optoelectronic system interacts photophysically with the skin [Figure 2I]. By recording the reflected light from the target area, biological information can be obtained[58]. At the same time, absorption and scattering make optical sensing possible. The battery-free wireless optoelectronic device in Figure 2J can monitor the temporal dynamics of heart rate and arterial blood flow using the backscattered light of the infrared (IR; 950 nm, AlGaAs) light-emitting diode (LED) of the silicon (PIN) photodetector[59], which can effectively monitor the systolic peak and dicrotic notch. The proper calibration of a device using standard oscillometric techniques for measuring diastolic and systolic pressures is crucial for accurately estimating mean arterial pressure (MAP), computed using:

$$MAP = P_{diastolic} + 0.33 \times (P_{systolic} + P_{diastolic}) \tag{4}$$

Which provides an estimate of the average arterial pressure throughout the cardiac cycle. It is approximately equal to the lower product of the arterial pressure curve divided by the duration of one heartbeat, averaged over several beats. The subsequent near field communication (NFC) wireless sampling rate of 25 Hz also provides sufficient resolution. The depth of detection is determined by the wavelength of light, and a 3 mm-thickness layer of the dermis and epidermis can block most of the photons from penetrating, so optimizing the wavelength can minimize absorption and improve penetration depth to the greatest extent possible.

Therefore, to achieve biomechanical monitoring of the cardiovascular system, pulse pressure wave analysis (PWA) and pulse transit time (PTT) are usually used[34]. In vascular stiffness illnesses, pulse wave velocity (PWV) is mostly assessed, which is directly connected to Young's modulus and hence the elastic modulus of the arterial wall[60,61]. PWV can also be measured non-invasively through a single heartbeat[62]. In addition, PTT is the time delay of pressure wave transmission between two parts of an artery[34].

$$PWV = \sqrt{\frac{Eh}{\rho d}} = \frac{L}{PTT}$$

$$BP = \alpha \cdot PWV^2 + \beta$$

Where d is the diameter of the tube, h is the thickness, ρ is the density and E is Young's modulus.

The artery's material qualities and shape dictate its α and β. Developing novel approaches for dynamically monitoring BP according to PTT or PWA necessitates the employment of additional algorithms or mathematical frameworks. As a result, accurate PWV or BP readings are necessary, which may be obtained by measuring pulse waves and heartbeats consistently. These findings indicate a strong foundation for technologies that can be applied across various fields, including both healthcare and non-healthcare applications.

Thermal transport
Compared to conventional techniques for measuring tissue flow, such as mechanical (plethysmography), optical [photoplethysmography, laser Doppler flowmetry (LDF) and laser speckle contrast imaging (LSCI)], acoustic (ultrasound), and thermal (various forms of heat removal), techniques based on heat transport have reduced sensitivity to motion[63]. Blood flow in tissue significantly affects the thermal response over time and space. This relationship allows for the determination of spatial variations in effective thermal conductivity, which, in turn, can indicate regional perfusion. Current non-invasive methods utilize metal heating and sensing plates [Figure 2K]. In the example of Figure 2L, an electronic microsystem strategy combined with thermal analysis techniques enables quantitative monitoring of near-surface blood flow velocity and direction to a depth of up to 2 mm[64]. The array consists of a single circular thermal actuator (10 nm Cr / 100 nm Au; 1.5 mm radius; 15 μm width) and two sensor rings (10 nm Cr / 100 nm Au; 0.5 mm radius) measuring the temperature difference between upstream and downstream flow. Each ring contains seven sensors (0.01 °C measurement accuracy, 2 Hz sampling rate, and response time of approximately 10 s) distributed around the ring at 45° intervals. For flow changes with a frequency of < 0.1 Hz, such as blood flow alternation related to myogenic activity of vascular smooth muscle (0.1 Hz), neurogenic activity of the vascular wall (0.04 Hz), and vascular endothelial influence (0.01 Hz), this platform can be used to measure blood flow changes very accurately.

This chapter introduces the latest developments in biological tissue mechanics sensing platforms, with a focus on the systematic features of engineering design and methods. Compared with conventional testing methods, microsystem techniques have demonstrated advantages such as sustainable monitoring, multi-signal acquisition, and the ability to apply live conditions in biological tissue mechanics testing. Table 1 summarizes the latest research results.

MECHANICAL EVALUATION WITH WIDE RANGE OF MEASUREMENT DEPTH FROM SUPERFICIAL SURFACE TO DEEP-TISSUE SENSING

Mechanical evaluation techniques that cover a wide range of measurement depths, from superficial surface to deep-tissue sensing, are crucial in various fields such as medicine, materials science, and

Table 1. A summary of recent advancements in sensing platforms for biological tissue mechanics

System	Sensing mechanisms	Advantages	Applications	Mechanism
Active vibration sensor[28,29,42]	Actuators generate mechanical vibrations; sensors detect the deformation caused by the wave propagation through tissues	Conformal contact with complex topography and other organ surfaces; quantitative real-time measurements and differentiation of abnormal tissues through injection	Assessment of moduli of body regions (lesion, normal); tumor tissue characterization	$\frac{V_{sensor}}{V_{actuator}} = \frac{e_{31}^2 A_{PZT} h_{PZT}}{k_{33} E_{PI} h_{PI} d^2} G\left(\frac{E_{tissue} d^3}{E_{PI} h_{PI}^3}\right)$
Ultrasonography [52,65-67]	Transducers generate and receive reflected ultrasonic waves from tissues with different acoustic impedances; the movement behavior of tissue can be measured based on the frequency shift of ultrasonic waves	Deep-tissue mapping with high spatial and temporal resolution based on wearable and stretchable arrays of ultrasonic transducers	Detection and visualization of deep-tissue signals (cardiac activity and central blood flow)	$V = \frac{c f_d}{2 f_0 \cos\theta}$
Stethoscope-based detector[29,41,68-70]	Mechanical vibrations from the human body are probed by piezoelectric, triboelectric materials or microphones to convert them to electrical signals	Detection of physiological signals in high sensitivity via nanostructured material; automated diagnoses of lung diseases	Continuous 10-hour seismo-cardiography monitoring; automated diagnoses of four types of lung diseases with about 95% accuracy	-
Strain gauge[55-57]	Deformation caused by external forces leads to a change in the resistance values, which derives from intrinsic characteristics of material or elaborately designed layout	Conformal devices with ultrahigh sensitivity to physiological signals (BP and heart rates) and applied forces (pressure and vibration)	Detection of long-term pressure wave and human motion; recognition of speech pattern	$E_s = \frac{3}{4}(1-v_s^2)F_{i-s} r_i^{-\frac{1}{2}} h_s^{-\frac{3}{2}}$
Optical illumination[58,59,71]	Light with wavelengths ranging from 400 to 500 nm penetrates the epidermis, while light exceeding 700 nm can reach deeper tissues beyond the dermis. The light reflected after biophysical interactions with the tissues provides important biological characteristic information, such as molecular content, morphology, and microstructure	Optical methods can provide real-time, continuous BP readings; continuous monitoring; reduced artifacts: optical measurements are less affected by motion artifacts	Monitoring the temporal dynamics of heart rate and arterial blood flow; quantifying tissue oxygenation and ultraviolet exposure; and performing four-color spectral assessments of skin condition	$MAP = P_{diastolic} + 0.33 \times (P_{systolic} + P_{diastolic})$
Thermal transport[63,64]	Central thermal actuators deliver a constant thermal driving source to create a mild, controlled temperature increase on the skin surface near the target vessel. Flow velocity can be inferred from the relative increase in temperature differences on either side	Executable spatial mapping; ability to track subtle or rapid temporal changes; assessment of natural, unaltered blood flow patterns; quantitative monitoring of near-surface blood flow velocity and direction; depth penetration of up to 2 mm; no external pressure application required; continuous monitoring capability; minimization of disturbances to the skin's natural temperature	Monitoring the near-surface microvascular system, including arterioles and capillary beds, with the ability to detect flow changes induced by deep breathing and palm-mediated congestion, as well as variations caused by skin urticaria	$\frac{\Delta Ts_{teady}}{T_{actuator}} = f3\left(\frac{L^2 v c_f \rho_f}{R \lambda_f}; \frac{\lambda_s}{\lambda_f}, \frac{h}{L}, \frac{B}{L}\right)$

BP: Blood pressure.

biomechanics[71,72]. Understanding the measurement depths associated with each method is crucial for selecting the appropriate technique based on the depth-dependent structures[2]. Figure 3A summarizes the different types of assessment methods for biological targets based on multiple measurement depths. A collection of some recent examples of sensing from surface to deep tissue, ranges from conformal sensing for evaluation of the elastic modulus of epidermis [Figure 3B and C][29] to an electromechanical device for characterization of biomechanics of deep tissue [Figure 3D and E][73], to an ultrasonic phased array for cardiac function assessment [Figure 3F and G][74], and to an ultrasound-on-chip (UoC) platform for whole body sensing [Figure 3H and I][65].

Measurement scale, including sensing depth, is a crucial parameter when using various methods for assessing depth-dependent structures in biological tissues. Figure 3A summarizes the microsystem
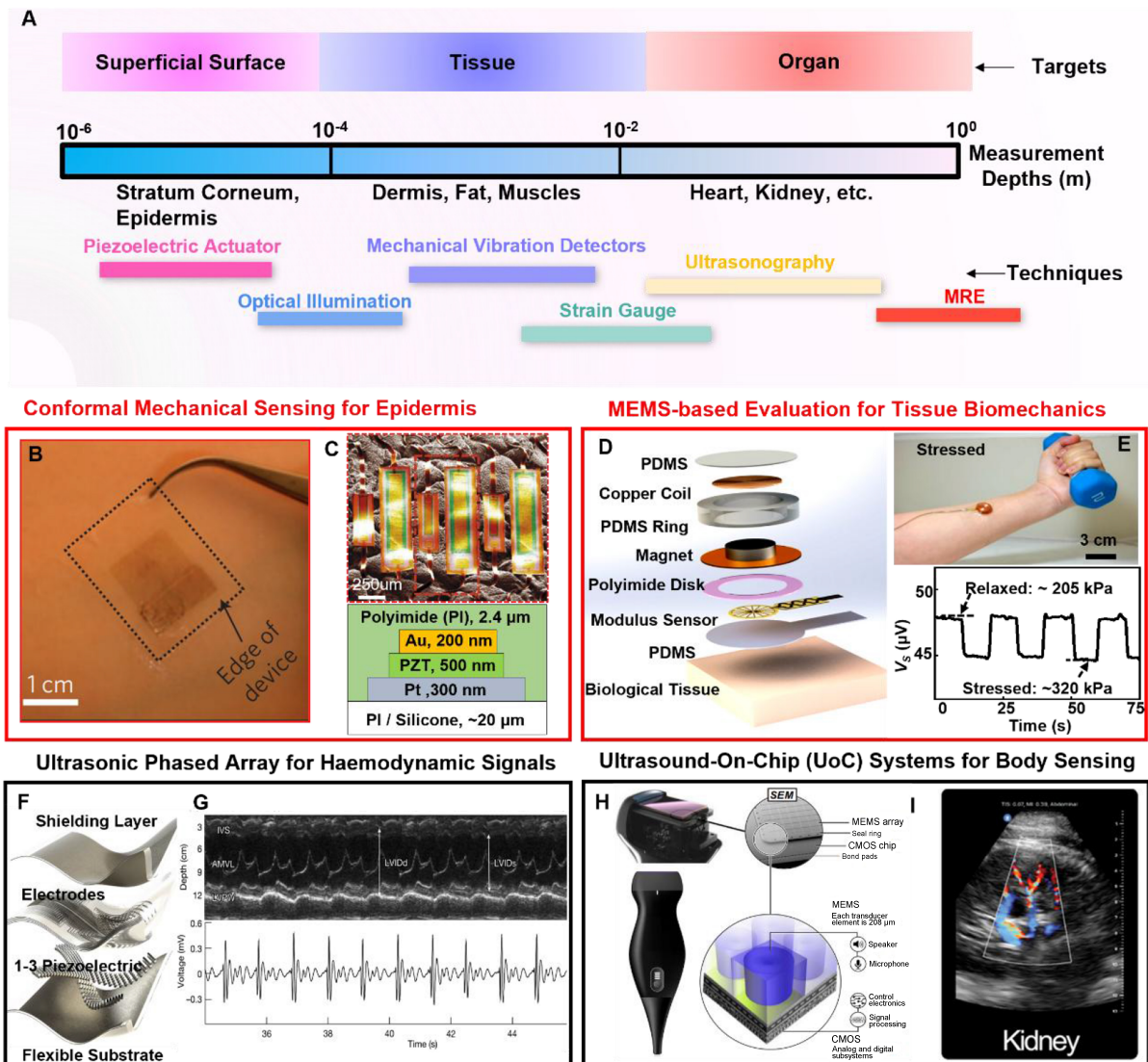
Figure 3. Mechanical evaluation with wide range of measurement depth from superficial surface to deep-tissue sensing. (A) Illustration of approximate dimensions of the measurement depths targeted to various biological targets via different types of evaluation methods, involving piezoelectric actuator, mechanical vibration detectors, optical illumination, strain gauge, ultrasonography and MRE, *etc*; (B) Photograph of a conformal sensing on a silicone sheet substrate for evaluation of the elastic modulus of epidermis. Reproduced with permission[29]. Copyright 2015, Springer Nature; (C) SEM image of the device on an artificial skin sample (upper). A cross-sectional illustration of the device (lower). Reproduced with permission[29]. Copyright 2015, Springer Nature; (D) Schematics showing the exploded view of a MEMS-based system for the characterization of tissue biomechanics. Reproduced with permission[73]. Copyright 2021, Springer Nature; (E) Dynamic monitoring of human body for modulus sensing. Upper: Photographs of devices on the forearm lifting a dumbbell. Lower: sensor Vs as function of time during monitoring. Reproduced with permission[73]. Copyright 2021, Springer Nature; (F) Exploded-view schematic illustration of the wearable imager for cardiac function assessment, with key elements in terms of 1-3 piezoelectric composite, electrodes and substrate. Reproduced with permission[74]. Copyright 2023, Springer Nature; (G) M-mode images (upper) extracted from wearable imager and corresponding ECG signals (lower). Reproduced with permission[74]. Copyright 2023, Springer Nature; (H) UoC designs for whole body sensing. Photos, SEM images, and schematic diagrams of an UoC design (left) equipped with 8960 MEMS transducers (upper right) on a CMOS chip, each enabled to send and receive ultrasound signals according to control/processing circuitry (lower right). Reproduced with permission[65]. Copyright 2021, American Chemical Society; (I) Example ultrasound imaging by the UoC, abdominal: vascular flow in kidney. Reproduced with permission[65]. Copyright 2021, American Chemical Society. MRE: Magnetic resonance elastography; SEM: scanning electron microscope; MEMS: micro-electromechanical system; Vs: voltages; AMVL: anterior mitral valve leaflet; LVPW: left ventricular posterior wall; LVIDd: left ventricular internal diameter end diastole; LVIDs: left ventricular internal diameter end systole; IVS: interventricular septum; ECG: electrocardiogram; UoC: ultrasound-on-chip; CMOS: complementary metal-oxide-semiconductor.

techniques with various measurement scales, from superficial surfaces to tissues and to organs. For example, optical illumination, mechanical vibration detectors, and strain gauges can be selected when measuring dermis, fat, and muscle tissues at the depths of 10^{-4}-10^{-2}, while piezoelectric actuators are suitable for superficial surfaces such as stratum corneum and epidermis. By utilizing appropriate measurement modalities and devices, the mechanical properties of biological tissues can be accurately characterized, leading to better understanding and potentially improved medical diagnosis and treatment.

The conformal modulus sensor (CMS) is a type of sensor used to measure the elastic modulus or stiffness of the targeted tissue surface because it can conform or adapt to various surfaces or objects being tested[20]. The sensor typically consists of active elements, such as strain gauges or piezoelectric materials, combined with the metal serpentine configurations providing electrical connectivity, resulting in a stretchable mechanical structure with a low modulus when held by a thin elastomer[29]. A representative example is shown in Figure 3B and C. The device provides a convenient and non-invasive method for coupling to the surface of the skin or other biological tissues using van der Waals forces, allowing for repeated use without sacrificing measurement accuracy [Figure 3B]. The conformal sensing attached to the artificial skin surface comprises seven actuators with sizes of 200 × 1,000 μm^2 and six sensors with sizes of 100 × 500 μm^2 (piezoelectric film, 500 nm thick) placed between two layers of serpentine configurations of metal traces (bottom: Ti/Pt, 20/300 nm; top: Cr/Au, 10/200 nm), with an encapsulation layer of PI [Figure 3C]. This conformal and piezoelectric device makes it possible to examine the viscoelasticity of biological tissues near the surface of the subject's epidermis and to map the mechanical features of the skin or other organs in space, which has a broad application prospect in therapeutic diagnosis and therapy of diseases[29,69]. Analyzing the data obtained from CMS applied to *ex vivo* skin samples provides valuable insights into the efficacy and mechanisms of action of moisturizing agents, as well as the relationship between hydration and skin properties. The directional and spatial mapping suggests that these devices can not only assess stiffness values but also provide information about the distribution of stiffness across different regions. This mapping capability allows for a detailed understanding of the mechanical properties of the skin in various areas, which can be important for the diagnosis and monitoring of early skin cancer[29].

The development and application of miniaturized electromagnetic (MEM) devices with vibratory actuators and soft strain-sensing sheets represent a promising advancement in the field of deep tissue characterization. They offer non-invasive, dynamic measurements of Young's modulus in skin and other soft tissues at depths ranging from approximately 1 to 8 mm, providing valuable insights for medical diagnostics, research, and treatment optimization. The electromechanical modulus (EMM) sensor described in Figure 3D is designed to capture the mechanical behavior of underlying soft tissue by applying periodic forces and measuring the resulting displacements[73]. It consists of two main components: a vibratory actuator and a strain-gauge sheet. The vibratory actuator located on the top layer (top coil, 200 μm) is responsible for generating a periodic Lorenz force with a fixed frequency applied to the tissue. The strain-gauge sheet in the form of serpentine metal traces (modulus sensor, ~2 μm) is used to measure the amplitude of displacement caused by applied forces. The total thickness of the device is ~2.5 mm and the contacting area is ~2 cm^2. Near-surface muscle tissue activity affects the modulus change, which can be measured with this EMM sensor [Figure 3E]. When the device is installed on the forearm, the forearm muscles contract to generate force to lift the dumbbell. The modulus values obtained through continuous recording of Vs changes over time suggest that the muscle tissue exhibits varying degrees of stiffness or elasticity during repeated iterations of movements. The modulus values of 205 and 320 kPa correspond to a relaxed state and a tensed state of muscle activity, respectively. Furthermore, the use of device arrays provides a powerful tool for obtaining detailed spatial and depth-wise information about the moduli of biological tissues. This information is invaluable for monitoring and diagnosing a range of health conditions.

A wearable ultrasound array capable of continuously capturing real-time images of the heart and assessing its function would be a remarkable advancement in the field of healthcare. The device combines several components: piezoelectric transducer arrays, composite electrodes of liquid metal, and encapsulation of triblock copolymer [Figure 3F][74]. Together, the anisotropic 1-3 piezoelectric composite and the silver-epoxy-based backing layer form a transducer element capable of sensing or actuation. Employing a smaller array pitch of 0.4 mm (0.78 ultrasonic wavelengths) in an ultrasonic imaging system can improve lateral resolution and reduce grating lobes. High-density multilayer stretchable electrodes (8 μm thick) based on a composite of eutectic gallium indium liquid metal and styrene-ethylene-butylene-styrene (SEBS) can provide a solution for individually addressing each element in a tight array. Incorporating electromagnetic shielding into ultrasound devices, such as using composite materials with great electromagnetic shielding properties, can help minimize the interference from external electromagnetic waves and maintain the integrity of ultrasonic RF signal, so as to improve the image quality. The described device possesses exceptional electromechanical properties, including low dielectric loss, wide bandwidth, a high electromechanical coupling coefficient, and negligible crosstalk, contributing to its excellent performance and versatility in various fields such as telecommunications, medical imaging, sensing technologies, and more. motion-mode (M-mode) imaging is a technique commonly used in medical ultrasound to monitor activities over time within a target region in one dimension[75]. It is particularly useful in cardiac imaging to evaluate the movement and functional properties of the heart. By analyzing the M-mode images, clinicians can assess various aspects of the motion of the target area, such as the one shown in Figure 3G, which extracts the primary targets in the M-type images including the left ventricular ventricle, the septum and the mitral/aortic valves from parasternal long-axis view B-mode images. The distance between feature boundaries, such as the thickness of myocardium and the diameter of left ventricular, can be tracked using M-mode. Analyzing the changes in the position of these boundaries over time, various measurements can be obtained to assess cardiac structure and function. Besides, it is possible to correlate mechanical exercises observed in M-mode visuals with the electrical signals recorded in an electrocardiogram (ECG) throughout various stages of the cardiac cycle (the lower inset of Figure 3G). This information helps in diagnosing cardiac abnormalities, evaluating heart function, and monitoring treatment progress.

Active semiconductor-based MEMS devices offer improved performance, miniaturization, integration, and adaptability compared to traditional measurement approaches, making them highly suitable for evaluating deep-tissue biomechanics, enabling more precise and efficient studies in biomedical applications. As shown in Figure 3H, the UoC integrated a two-dimensional array of 8,690 MEMS transducers in a 140 × 64 configuration (area of 30 mm × 13.3 mm, spacing pitch of 200 μm) with complementary metal-oxide-semiconductor (CMOS) control and processing electronics has significant potential for development as an inexpensive whole body imaging probe[65]. By combining a UoC platform with a portable system and an artificial intelligence system, it becomes possible to perform quantitative measurements and obtain high-quality clinical visuals of deep tissues throughout the human body, such as the abdominal UoC ultrasound image: blood vessel flow in the kidney shown in Figure 3I. Excitingly, the proliferation of portable and low-cost ultrasound imaging has the potential to revolutionize global health and make a significant impact on the fields of medicine.

CLINICAL APPLICATIONS OF WEARABLE DEVICES FOR TISSUE MECHANICS CHARACTERIZATION

Assessment of biological tissue mechanics across multiple dimensions offers a wealth of human-computer interaction applications and clinical practices. This multidimensional analysis can lead to improvements in

various areas, including diagnostics, personalized medicine, treatment strategies, and rehabilitation techniques. Here, examples include voice code recognition based on ferroelectric nanogenerator (FENG) microphone [Figure 4A][41], dermatologic malignancy evaluation using CMS system [Figure 4B][29], arterial stiffness measurement via a conformal ultrasonic device [Figure 4C][20], tumor volume regression sensing by flexible autonomous sensors (FAST) [Figure 4D][76], and physiological monitoring for hospital neonatal care by a wireless limb unit [Figure 4E][77].

The application of wearable and portable devices in our daily lives necessitates continuous innovation in human-computer interaction technology[78]. These advancements aim to make devices more intuitive, responsive, and seamlessly integrated into everyday routines. However, the push for such innovation inevitably brings challenges, especially concerning personal privacy and information security. As shown in Figure 4A, given the flexibility and wearability of FENG, the FENG device can be installed in a wearable device or personal computer. The high sensitivity of the FENG-based microphone allows speech recognition, which provides multiple layers of security for the authentication system[41]. When an unauthorized user makes an access request, the generated voltage reflects the time-domain acoustic information. FENG devices analyze the voiceprint information and accurately reveal the user's identity, preventing unauthorized users from accessing the owner's personal computer, even in the case of an unauthorized user obtaining the correct speech code. Moreover, these advantages can contribute to the development of new-style loudspeakers and the improvement of active noise cancellation technology in various domains, making audio systems more efficient, compact, and capable of delivering high-quality sound[70].

Stiffness variations in tissues can be indicative of underlying health conditions, such as abnormalities or disease[13]. Therefore, mapping these stiffness differences can provide valuable insights for medical diagnostics and monitoring. Here, by utilizing reversible soft contact, the CMS [Figure 4A and B] consisting of ultrathin, stretchable networks of mechanical actuators and sensors can assess the stiffness of different regions on the skin. Figure 4B presents the image of a piezoelectric device mounted on the forearm for mapping the lesion regions of dermatologic malignancy and the spatial mapping of modulus[29]. *In vivo* modulus measurement results of the forearm indicate that the modulus in the pathological region is higher than that in the healthy region. Mapping the mechanical properties of the skin can provide valuable information for the diagnosis and monitoring of early skin cancer.

Monitoring the central BP (CBP) waveform representing the pressure exerted by the blood on the walls of the central arteries provides valuable insights into the hemodynamic status of an individual and can help in the early detection of cardiovascular abnormalities[79]. Figure 4C on the left shows a conformal ultrasound device attached to the central vessel pulsation in deep tissues, including the CA (subcutaneous about 25 mm) and internal jugular veins (int. JV) and external jugular veins (ext. JV) for high-precision measurement of the behavior of the central vessel pulsation[20]. The CA is a major blood vessel located in the neck, responding by supplying oxygenated blood to the head and neck region, including the brain. The int. JV drains deoxygenated blood from the brain, face, and neck and carries it back to the right atrium of the heart. Another example is the simultaneous measurement of ECG and BP of the brachial artery (BA), as shown on the right in Figure 4C. PWV is used to assess arterial stiffness with a value of 5.4 m·s^{-1}, consistent with commercial devices. The conformal and stretchable ultrasound device can be used to collect a series of essential characteristics of central blood vessels, such as their structure, blood flow dynamics, and any abnormalities or pathologies present.
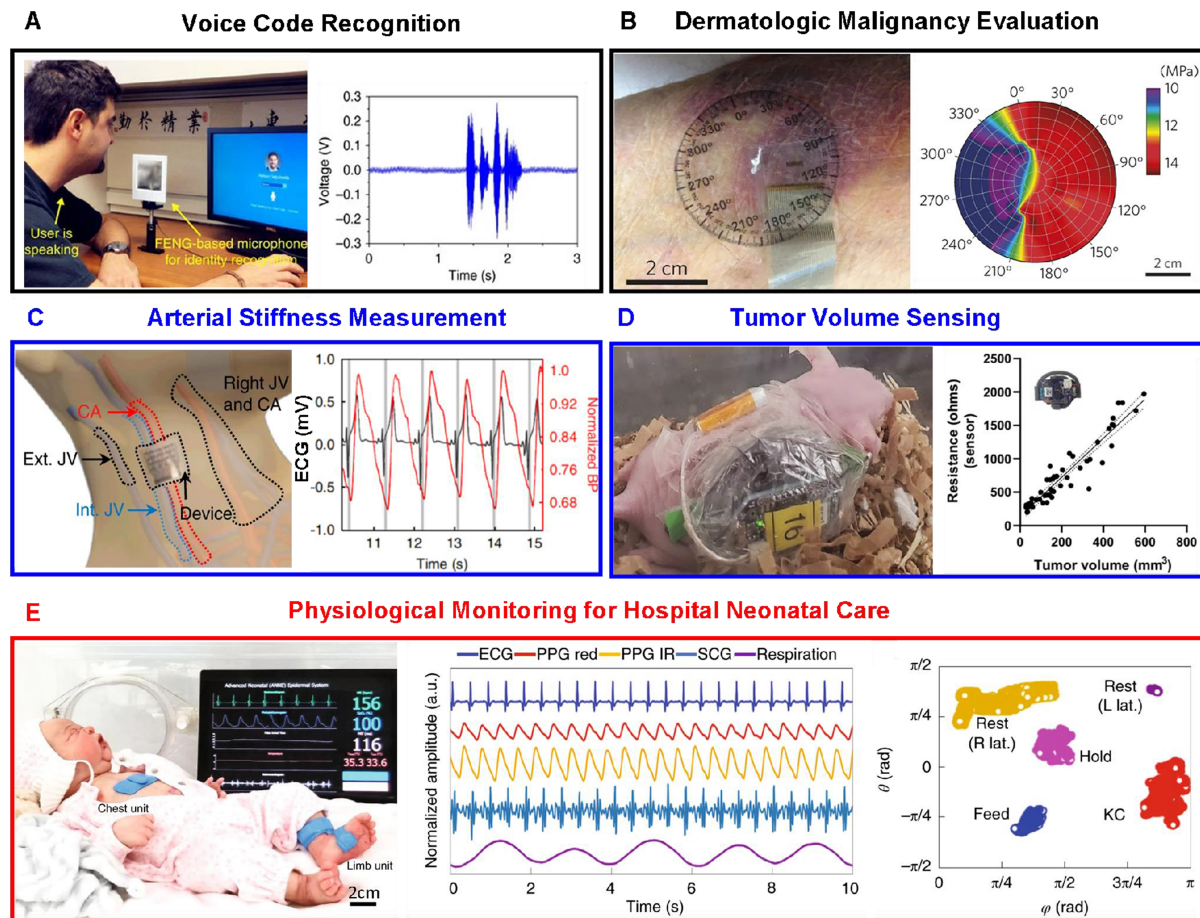
Figure 4. Clinical applications of wearable devices for tissue mechanics characterization. (A) Left: User request access using FENG-based microphone for voice code recognition. Right: Sound wave of voice code. Reproduced with permission[41]. Copyright 2017, Springer Nature; (B) Left: Photographs of a piezoelectric device mounted on the forearm to map the lesion regions of dermatologic malignancy. Right: Spatial mapping of modulus corresponding to measurements on the forearm. Reproduced with permission[29]. Copyright 2015, Springer Nature; (C) Left: Illustration of the ultrasound sensor mounted on the neck for measurement of pulse waveform from CA, external jugular vein (ext. JV) and internal jugular vein (int. JV). Right: pulse waveforms of ECG and BP at the artery to assess vascular stiffness accessibly and reliably. Reproduced with permission[20]. Copyright 2018, Springer Nature; (D) Left: Photographs of an autonomous sensor holding on the mouse. Right: Closely correlation between resistance readouts from the sensor and the tumor volume. Reproduced with permission[76]. Copyright 2022, American Association for the Advancement of Science; (E) Left: Photograph of the device (chest and limb units) on a neonate in a NICU isolette, with exemplary data displaying on a user interface. Middle: Representative data collected by chest and limb units. Right: Rotational angles between the device and reference frames for a neonate in NICU in different body positions. Reproduced with permission[77]. Copyright 2020, Springer Nature. FENG: Ferroelectric nanogenerator; CA: carotid artery; ECG: electrocardiogram; BP: blood pressure; NICU: neonatal intensive care unit.

In the field of oncology research, the process of clinical translation involves testing thousands of potential cancer drugs to identify the few that are suitable for use in patients. Researchers are exploring the use of tools that automate *in vivo* tumor regression measurements. These tools gather high-resolution continuous datasets from larger animal cohorts, providing more robust and detailed information. Here, FAST mounted comfortably on the mouse can be pre-stretched to 50% of their original length and have a sensitive strain range of 25% to 75%, which means they are capable of precisely measuring changes in tumor volume within a certain strain range[76]. The correlation between FAST sensor resistance readouts and tumor volume measurements obtained through calipers indicates a strong relationship between the two variables. This suggests that the resistance readouts from the FAST sensor can serve as a reliable indicator of tumor volume *in vivo* [Figure 4D]. Real-time tumor regression datasets have the potential to significantly enhance the

screening of cancer therapies *in vivo*. By providing immediate and dynamic information on tumor response to treatment, these datasets can expedite and automate the process, leading to more efficient and effective cancer therapy development.

Skin interface biosensors for advanced wireless physiological monitoring in neonatal and pediatric intensive care units (NICUs and PICUs, respectively) are designed to be non-invasive, comfortable for patients[80], providing real-time monitoring of various physiological parameters, with the potential to greatly improve patient care and outcomes. Figure 4E exhibits a photograph of the chest and limb units on a model of a neonate in a NICU isolation unit, with exemplary data displayed on a user interface[59]. These exemplary data, for instance, ECGs, photoplethysmograms (PPGs), seismocardiograms (SCGs), and chest movements obtained from a neonate with a gestational age (GA) of 29 weeks, are captured through uninterrupted wireless transmission to a mobile tablet utilizing using a platform with an embedded batter. The real-time signal analysis algorithms executed on the mobile tablet enable the transmitted raw data from the devices to be processed immediately. This allows dynamic and adaptive vital signs to be displayed with minimal time delay. Additional clinically important data, such as the differences in rotational angles between devices and reference frames during resting (left and right lateral position), holding, feeding, and kangaroo care (KC) events for a neonate in NICU, are exhibited on the right in Figure 4E. This multifunctional system has the potential to greatly improve the quality of neonatal and pediatric intensive care.

CONCLUSION AND PERSPECTIVES

Collectively, these advancements in materials science, device engineering, and measurement principles have led to the development of high-precision measurement systems for the mechanical characterization of soft biological tissues. These systems enable researchers to study tissue mechanics in a controlled and quantitative manner, providing insights into the behavior and properties of tissues under physiological and pathological conditions. In this review, we review the recent advancements in sensing platforms for biological tissue mechanics, including the measurement mechanism and engineering design, and the applications in tissue engineering, biomedical research and clinical medicine. The emphasis is on the systematic characteristics of engineering designs and methods that have diagnostic utility across different measurement depths. The latest research results are summarized in Table 1. The biological tissue mechanics sensing platforms feature unique modes of interface with soft tissue, high measurement resolutions and wider application ranges, which cannot be supported by traditional methods. Selecting the appropriate mechanical sensing platforms according to the sensing needs of tissues or organs with different depths such as vocal cord vibration, cardiac beating, tissue stiffness and arterial pulsation can provide a rich application of clinical medicine. However, the development of a single, scalable measurement system with hybrid functions for evaluating biomechanics at multiple spatial scales and depths in a rapid, precise, and non-invasive manner is a persistent challenge.

To address this challenge, researchers and engineers are exploring different approaches and technologies: (1) Advances in imaging technologies, such as MRI, ultrasound, and optical coherence tomography (OCT), have enabled non-invasive visualization of tissues and structures at various scales. The wearable ultrasonic transducer arrays, for example, are used for deep tissue sensing (> 10 cm) at a spatial resolution of hundreds of micrometers[20]. These imaging techniques can provide valuable information about biomechanical properties, such as tissue elasticity and deformation, without requiring invasive procedures; (2) Combining multiple sensors and measurement devices can help capture biomechanical data at different scales. For instance, incorporating pressure sensors, strain gauges, accelerometers, and force plates into a single system can provide a more comprehensive understanding of biomechanical behavior. Integration of these sensors with imaging technologies allows for simultaneous data acquisition and correlation[81]; (3) Computational

models, such as finite element analysis (FEA) and multibody dynamics simulations, can simulate biomechanical behavior based on known anatomical and mechanical properties. These models can be calibrated and validated using experimental data obtained from non-invasive measurements. By combining computational modeling with experimental measurements, researchers can gain insights into biomechanical processes at various scales. For example, a MEM device integrating a vibration actuator and a soft strain sensor is used to dynamically measure Young's modulus of skin and other soft tissues. FEA is used to quantify the mechanical coupling between actuators, sensors and tissues[73]; (4) The development of miniaturized and wireless sensors offers the potential for unobtrusive and continuous monitoring of biomechanics *in vivo*. These sensors can be implanted, attached to the skin, or even ingested to collect data on parameters such as strain, pressure, and motion. Advancements in flexible and stretchable electronics have facilitated the integration of such sensors with the human body. A typical example is a contact lens with a fully integrated system that can operate wirelessly, battery-free, while detecting and transmitting intraocular pressure to a mobile phone via standard NFC technology[10]; (5) Machine learning algorithms and artificial intelligence techniques can assist in processing and analyzing large datasets generated by hybrid measurement systems. These algorithms can identify patterns, predict behavior, and extract meaningful information from complex biomechanical data, aiding in the development of more precise and efficient evaluation methods. For instance, Kim *et al.* used algorithms to classify EMG signals[82]. With machine learning algorithms, soft electronics are increasingly intelligent and can achieve real-time analysis and diagnosis.

The complexity and diversity of biological systems requires collaboration among diverse scientific disciplines, including biology, chemistry, physics, and computer science. Innovating flexible wearables for assessing the biomechanical properties of deep tissues is crucial for broader disease assessment. These advancements will not only enhance current research but also facilitate future exploratory studies and clinical applications.

DECLARATIONS

Authors' contributions
Investigation, visualization, writing - original draft: Lu Y
Writing - original draft: Ma L
Investigation, visualization, data curation: Zhang H
Data curation: Mei Y, Xiong Z
Conceptualization, methodology, resources, supervision, writing - review and editing: Song E

Availability of data and materials
Not applicable.

Conflicts of interest
All authors declare that there are no conflicts of interest.

Ethical approval and consent to participate

Not applicable.

Consent for publication

Not applicable.

Copyright

© The Author(s) 2024.

REFERENCES

1. Gómez-González M, Latorre E, Arroyo M, Trepat X. Measuring mechanical stress in living tissues. *Nat Rev Phys* 2020;2:300-17. DOI

2. Guimarães CF, Gasperini L, Marques AP, Reis RL. The stiffness of living tissues and its implications for tissue engineering. *Nat Rev Mater* 2020;5:351-70. DOI

3. Lyu Q, Gong S, Yin J, Dyson JM, Cheng W. Soft wearable healthcare materials and devices. *Adv Healthc Mater* 2021;10:e2100577. DOI PubMed

4. Chanda A, Singh G. Hyperelastic models for anisotropic tissue characterization. In: Mechanical properties of human tissues. Singapore: Springer Nature;2023. pp.73-83. DOI

5. Yazdi SJM, Baqersad J. Mechanical modeling and characterization of human skin: a review. *J Biomech* 2022;130:110864. DOI

6. Chen S, Sun L, Zhou X, et al. Mechanically and biologically skin-like elastomers for bio-integrated electronics. *Nat Commun* 2020;11:1107. DOI

7. Liu S, Rao Y, Jang H, Tan P, Lu N. Strategies for body-conformable electronics. *Matter* 2022;5:1104-36. DOI

8. Zhao Y, Zhang S, Yu T, et al. Ultra-conformal skin electrodes with synergistically enhanced conductivity for long-time and low-motion artifact epidermal electrophysiology. *Nat Commun* 2021;12:4880. DOI PubMed PMC

9. Gogurla N, Kim Y, Cho S, Kim J, Kim S. Multifunctional and ultrathin electronic tattoo for on-skin diagnostic and therapeutic applications. *Adv Mater* 2021;33:e2008308. DOI PubMed

10. Kim J, Park J, Park YG, et al. A soft and transparent contact lens for the wireless quantitative monitoring of intraocular pressure. *Nat Biomed Eng* 2021;5:772-82. DOI PubMed

11. Silva F, Lira M. Intraocular pressure measurement: a review. *Surv Ophthalmol* 2022;67:1319-31. DOI PubMed

12. Chen C, Cheng Y, Zhu X, et al. Ultrasound assessment of skin thickness and stiffness: the correlation with histology and clinical score in systemic sclerosis. *Arthritis Res Ther* 2020;22:197. DOI PubMed PMC

13. Villalobos Lizardi JC, Baranger J, Nguyen MB, et al. A guide for assessment of myocardial stiffness in health and disease. *Nat Cardiovasc Res* 2022;1:8-22. DOI PubMed

14. Elouneg A, Chambert J, Lejeune A, Lucot Q, Jacquet E, Bordas SPA. Anisotropic mechanical characterization of human skin by in vivo multi-axial ring suction test. *J Mech Behav Biomed Mater* 2023;141:105779. DOI PubMed

15. Pissarenko A, Meyers MA. The materials science of skin: analysis, characterization, and modeling. *Prog Mater Sci* 2020;110:100634. DOI

16. Zhao Y, Feng B, Lee J, Lu N, Pierce DM. A multi-layered computational model for wrinkling of human skin predicts aging effects. *J Mech Behav Biomed Mater* 2020;103:103552. DOI PubMed

17. Wells RG. Tissue mechanics and fibrosis. *Biochim Biophys Acta* 2013;1832:884-90. DOI PubMed PMC

18. Hu H, Ma Y, Gao X, et al. Stretchable ultrasonic arrays for the three-dimensional mapping of the modulus of deep tissue. *Nat Biomed Eng* 2023;7:1321-34. DOI PubMed

19. Sack I. Magnetic resonance elastography from fundamental soft-tissue mechanics to diagnostic imaging. *Nat Rev Phys* 2023;5:25-42. DOI

20. Wang C, Li X, Hu H, et al. Monitoring of the central blood pressure waveform via a conformal ultrasonic device. *Nat Biomed Eng* 2018;2:687-95. DOI PubMed PMC

21. Hiscox LV, Schwarb H, McGarry MDJ, Johnson CL. Aging brain mechanics: progress and promise of magnetic resonance elastography. *Neuroimage* 2021;232:117889. DOI PubMed PMC

22. Zhao C, Park J, Root SE, Bao Z. Skin-inspired soft bioelectronic materials, devices and systems. *Nat Rev Bioeng* 2024;2:671-90. DOI

23. Feiner R, Dvir T. Tissue–electronics interfaces: from implantable devices to engineered tissues. *Nat Rev Mater* 2018;3:17076. DOI

24. Li J, Carlos C, Zhou H, et al. Stretchable piezoelectric biocrystal thin films. *Nat Commun* 2023;14:6562. DOI PubMed PMC

25. Sunwoo S, Han SI, Park CS, et al. Soft bioelectronics for the management of cardiovascular diseases. *Nat Rev Bioeng* 2024;2:8-24. DOI

26. Dai Y, Hu H, Wang M, Xu J, Wang S. Stretchable transistors and functional circuits for human-integrated electronics. *Nat Electron* 2021;4:17-29. DOI

27. Ryu H, Park Y, Luan H, et al. Transparent, compliant 3D mesostructures for precise evaluation of mechanical characteristics of organoids. *Adv Mater* 2021;33:e2100026. DOI PubMed PMC

28. Yu X, Wang H, Ning X, et al. Needle-shaped ultrathin piezoelectric microsystem for guided tissue targeting via mechanical sensing.

Nat Biomed Eng 2018;2:165-72. DOI PubMed

29.   Dagdeviren C, Shi Y, Joe P, et al. Conformal piezoelectric systems for clinical and experimental characterization of soft tissue biomechanics. *Nat Mater* 2015;14:728-36. DOI PubMed

30.   Kennedy KM, Chin L, McLaughlin RA, et al. Quantitative micro-elastography: imaging of tissue elasticity using compression optical coherence elastography. *Sci Rep* 2015;5:15538. DOI PubMed PMC

31.   Kim J, Salvatore GA, Araki H, et al. Battery-free, stretchable optoelectronic systems for wireless optical characterization of the skin. *Sci Adv* 2016;2:e1600418. DOI PubMed PMC

32.   Pirnat G, Marinčič M, Ravnik M, Humar M. Quantifying local stiffness and forces in soft biological tissues using droplet optical microcavities. *Proc Natl Acad Sci U S A* 2024;121:e2314884121. DOI PubMed PMC

33.   Hsu CK, Lin HH, Harn HI, Hughes MW, Tang MJ, Yang CC. Mechanical forces in skin disorders. *J Dermatol Sci* 2018;90:232-40. DOI PubMed

34.   Janmey PA, Miller RT. Mechanisms of mechanical signaling in development and disease. *J Cell Sci* 2011;124:9-18. DOI PubMed PMC

35.   Kuzum D, Takano H, Shim E, et al. Transparent and flexible low noise graphene electrodes for simultaneous electrophysiology and neuroimaging. *Nat Commun* 2014;5:5259. DOI PubMed PMC

36.   Kim GH, Kim K, Nam H, et al. CNT-Au nanocomposite deposition on gold microelectrodes for improved neural recordings. *Sensor Actuat B Chem* 2017;252:152-8. DOI

37.   Fang H, Yu KJ, Gloschat C, et al. Capacitively coupled arrays of multiplexed flexible silicon transistors for long-term cardiac electrophysiology. *Nat Biomed Eng* 2017;1:0038. DOI PubMed PMC

38.   Viventi J, Kim DH, Moss JD, et al. A conformal, bio-interfaced class of silicon electronics for mapping cardiac electrophysiology. *Sci Transl Med* 2010;2:24ra22. DOI PubMed PMC

39.   Viventi J, Kim DH, Vigeland L, et al. Flexible, foldable, actively multiplexed, high-density electrode array for mapping brain activity in vivo. *Nat Neurosci* 2011;14:1599-605. DOI PubMed PMC

40.   Won SM, Cai L, Gutruf P, Rogers JA. Wireless and battery-free technologies for neuroengineering. *Nat Biomed Eng* 2023;7:405-23. DOI PubMed PMC

41.   Li W, Torres D, Díaz R, et al. Nanogenerator-based dual-functional and self-powered thin patch loudspeaker or microphone for flexible electronics. *Nat Commun* 2017;8:15310. DOI PubMed PMC

42.   Turner BL, Senevirathne S, Kilgour K, et al. Ultrasound-powered implants: a critical review of piezoelectric material selection and applications. *Adv Healthc Mater* 2021;10:e2100986. DOI PubMed

43.   Zheng Q, Tang Q, Wang ZL, Li Z. Self-powered cardiovascular electronic devices and systems. *Nat Rev Cardiol* 2021;18:7-21. DOI PubMed

44.   Moin A, Zhou A, Rahimi A, et al. A wearable biosensing system with in-sensor adaptive machine learning for hand gesture recognition. *Nat Electron* 2021;4:54-63. DOI

45.   Lee K, Ni X, Lee JY, et al. Mechano-acoustic sensing of physiological processes and body motions via a soft wireless device placed at the suprasternal notch. *Nat Biomed Eng* 2020;4:148-58. DOI PubMed PMC

46.   Song H, Luo G, Ji Z, et al. Highly-integrated, miniaturized, stretchable electronic systems based on stacked multilayer network materials. *Sci Adv* 2022;8:eabm3785. DOI PubMed PMC

47.   Kim T, Shin Y, Kang K, et al. Ultrathin crystalline-silicon-based strain gauges with deep learning algorithms for silent speech interfaces. *Nat Commun* 2022;13:5815. DOI PubMed PMC

48.   Lopez CAS. Advanced materials towards flexible printable bioelectronics, bioenergy devices and medical devices. 2021. Available from: https://www.proquest.com/openview/d150170f25f57f6a15d5c794a2ce5435/1?pq-origsite=gscholar&cbl=18750&diss=y. [Last accessed on 19 Oct 2024].

49.   Choi S, Han SI, Kim D, Hyeon T, Kim DH. High-performance stretchable conductive nanocomposites: materials, processes, and device applications. *Chem Soc Rev* 2019;48:1566-95. DOI PubMed

50.   Zhang L, Du W, Kim JH, Yu CC, Dagdeviren C. An emerging era: conformable ultrasound electronics. *Adv Mater* 2024;36:e2307664. DOI PubMed

51.   Lin M, Hu H, Zhou S, Xu S. Soft wearable devices for deep-tissue sensing. *Nat Rev Mater* 2022;7:850-69. DOI

52.   Wang C, Qi B, Lin M, et al. Continuous monitoring of deep-tissue haemodynamics with stretchable ultrasonic phased arrays. *Nat Biomed Eng* 2021;5:749-58. DOI PubMed

53.   Gill RW. Measurement of blood flow by ultrasound: accuracy and sources of error. *Ultrasound Med Biol* 1985;11:625-41. DOI PubMed

54.   Nayeem MOG, Lee S, Jin H, et al. All-nanofiber-based, ultrasensitive, gas-permeable mechanoacoustic sensors for continuous long-term heart monitoring. *Proc Natl Acad Sci U S A* 2020;117:7063-70. DOI PubMed PMC

55.   Cui Z, Wang W, Guo L, et al. Haptically quantifying Young's modulus of soft materials using a self-locked stretchable strain sensor. *Adv Mater* 2022;34:e2104078. DOI PubMed

56.   Fan X, Forsberg F, Smith AD, et al. Graphene ribbons with suspended masses as transducers in ultra-small nanoelectromechanical accelerometers. *Nat Electron* 2019;2:394-404. DOI

57.   Cai P, Hu B, Leow WR, et al. Biomechano-interactive materials and interfaces. *Adv Mater* 2018;30:e1800572. DOI PubMed

58.   Lee GH, Moon H, Kim H, et al. Multifunctional materials for implantable and wearable photonic healthcare devices. *Nat Rev Mater*

2020;5:149-65. DOI PubMed PMC

59. Choi J, Ghaffari R, Baker LB, Rogers JA. Skin-interfaced systems for sweat collection and analytics. *Sci Adv* 2018;4:eaar3921. DOI PubMed PMC

60. Magder S. The meaning of blood pressure. *Crit Care* 2018;22:257. DOI PubMed PMC

61. Ma SP, Vunjak-Novakovic G. Tissue-engineering for the study of cardiac biomechanics. *J Biomech Eng* 2016;138:021010. DOI PubMed PMC

62. Macgowan CK, Henkelman RM, Wood ML. Pulse-wave velocity measured in one heartbeat using MR tagging. *Magn Reson Med* 2002;48:115-21. DOI PubMed

63. Webb RC, Ma Y, Krishnan S, et al. Epidermal devices for noninvasive, precise, and continuous mapping of macrovascular and microvascular blood flow. *Sci Adv* 2015;1:e1500701. DOI PubMed PMC

64. Kwon K, Kim JU, Deng Y, et al. An on-skin platform for wireless monitoring of flow rate, cumulative loss and temperature of sweat in real time. *Nat Electron* 2021;4:302-12. DOI

65. Rothberg JM, Ralston TS, Rothberg AG, et al. Ultrasound-on-chip platform for medical imaging, analysis, and collective intelligence. *Proc Natl Acad Sci U S A* 2021;118:e2019339118. DOI PubMed PMC

66. Hu H, Hu C, Guo W, Zhu B, Wang S. Wearable ultrasound devices: an emerging era for biomedicine and clinical translation. *Ultrasonics* 2024;142:107401. DOI PubMed

67. Pang DC, Chang CM. Development of a novel transparent flexible capacitive micromachined ultrasonic transducer. *Sensors* 2017;20:1443. DOI

68. Zang J, Zhou C, Xiang M, et al. Optimum design and test of a novel bionic electronic stethoscope based on the cruciform microcantilever with leaf microelectromechanical systems structure. *Adv Mater Technol* 2022;7:2101501. DOI

69. Nguyen TD, Deshmukh N, Nagarah JM, et al. Piezoelectric nanoribbons for monitoring cellular deformations. *Nat Nanotechnol* 2012;7:587-93. DOI

70. Wang W, Jiang Y, Thomas PJ. Structural design and physical mechanism of axial and radial sandwich resonators with piezoelectric ceramics: a review. *Sensors* 2021;21:1112. DOI PubMed PMC

71. Kaltenbrunner M, Sekitani T, Reeder J, et al. An ultra-lightweight design for imperceptible plastic electronics. *Nature* 2013;499:458-63. DOI PubMed

72. Joodaki H, Panzer MB. Skin mechanical properties and modeling: a review. *Proc Inst Mech Eng H* 2018;232:323-43. DOI PubMed

73. Song E, Xie Z, Bai W, et al. Miniaturized electromechanical devices for the characterization of the biomechanics of deep tissue. *Nat Biomed Eng* 2021;5:759-71. DOI PubMed

74. Hu H, Huang H, Li M, et al. A wearable cardiac ultrasound imager. *Nature* 2023;613:667-75. DOI PubMed PMC

75. Feigenbaum H. Role of M-mode technique in today's echocardiography. *J Am Soc Echocardiogr* 2010;23:240-57. DOI PubMed

76. Abramson A, Chan CT, Khan Y, et al. A flexible electronic strain sensor for the real-time monitoring of tumor regression. *Sci Adv* 2022;8:eabn6550. DOI PubMed PMC

77. Chung HU, Rwei AY, Hourlier-Fargette A, et al. Skin-interfaced biosensors for advanced wireless physiological monitoring in neonatal and pediatric intensive-care units. *Nat Med* 2020;26:418-29. DOI PubMed PMC

78. MacKenzie IS. Human-computer interaction: an empirical research perspective. 2nd edition. 2024. Available from: https://shop.elsevier.com/books/human-computer-interaction/mackenzie/978-0-443-14096-9. [Last accessed on 19 Oct 2024].

79. Bakogiannis C, Stavropoulos K, Papadopoulos C, Papademetriou V. The impact of various blood pressure measurements on cardiovascular outcomes. *Curr Vasc Pharmacol* 2021;19:313-22. DOI PubMed

80. Adegboro CO, Choudhury A, Asan O, Kelly MM. Artificial intelligence to improve health outcomes in the NICU and PICU: a systematic review. *Hosp Pediatr* 2022;12:93-110. DOI PubMed

81. Lee JH, Cho K, Kim JK. Age of flexible electronics: emerging trends in soft multifunctional sensors. *Adv Mater* 2024;36:e2310505. DOI PubMed

82. Kim DH, Lu N, Ma R, et al. Epidermal electronics. *Science* 2011;333:838-43. DOI